

Research

Effects of forming techniques on residual stresses in stiffening ribs of sandwich panels

Raheem Al-Sabur¹ · Andrzej Kubit² · Hassanein I. Khalaf¹ · Kamil Ochał³ · Andrzej Gradzik³ · Marcin Korzeniowski⁴ · Ján Slota⁵

Received: 22 September 2023 / Accepted: 15 December 2023

Published online: 20 January 2024

© The Author(s) 2024 [OPEN](#)

Abstract

This study investigates residual stresses in stiffening ribs of composite materials formed by stamping in a punch-die system. Using two-dimensional X-ray diffraction (XRD), we measured residual stresses on both the anterior and posterior sides. Three LITECOR[®] composite types, with core thicknesses of 0.8, 1.25, and 1.6 mm, were examined. Results indicate that as core thickness increases, residual stress values decrease on both sides. Notably, anterior side stresses on the y-axis are relatively higher (1027–1199 MPa) compared to the x-axis, exceeding posterior side values (998–1083 MPa) at 0.8 mm core thickness. Moreover, the study compares these values with Single Point Incremental Forming (SPIF) and finds that SPIF generally yields lower stress values for all core thicknesses. These findings suggest that SPIF is favourable for achieving minimal residual stress in LITECOR[®] composites. Addressing residual stresses is crucial for enhancing structural integrity and extending the service life of sandwich panels and composite materials.

Article highlights

1. *Residual stresses in stiffening ribs* Examined the distribution of residual stresses in composite material stiffening ribs formed by stamping, highlighting their significant impact on structural integrity.
2. *Core thickness influence* Demonstrated that increasing the core thickness reduces residual stress values, emphasizing the role of core thickness in controlling residual stresses.
3. *SPIF versus stamping* Compared two forming methods and found that Single Point Incremental Forming (SPIF) results in lower residual stress, suggesting its suitability for achieving minimal residual stress in LITECOR[®] composites.

Keywords Residual stresses · Stamping method · Single point incremental · X-ray diffraction · LITECOR[®]

✉ Andrzej Kubit, akubit@prz.edu.pl; Raheem Al-Sabur, raheem.musawel@uobasrah.edu.iq; Hassanein I. Khalaf, hassanein.khalaf@uobasrah.edu.iq; Kamil Ochał, kochal@prz.edu.pl; Andrzej Gradzik, andrzej_gradzik@prz.edu.pl; Marcin Korzeniowski, marcin.korzeniowski@pwr.edu.pl; Ján Slota, jan.slota@tuke.sk | ¹Mechanical Department, Engineering College, University of Basrah, Basrah, Iraq. ²Department of Manufacturing and Production Engineering, Faculty of Mechanical Engineering and Aeronautics, Rzeszow University of Technology, Al. Powst. Warszawy 8, 35-959 Rzeszow, Poland. ³Department of Materials Science, Faculty of Mechanical Engineering and Aeronautics, Rzeszow University of Technology, Al. Powst. Warszawy 8, 35-959 Rzeszow, Poland. ⁴Department of Metal Forming, Welding and Metrology, Faculty of Mechanical Engineering, Wrocław University of Science and Technology, Wyb. Wyspińskiego 27, 50-370 Wrocław, Poland. ⁵Institute of Technology and Materials Engineering, Technical University of Košice, 040 01 Kosice, Slovakia.



1 Introduction

In the last decade, sandwich panels have evolved significantly, especially in applications where lightweight is essential [1]. Sandwich panels usually have three layers: a core in the middle and two layers of rigid material where the face materials offer strength and longevity, while the core material contributes to the panel's rigidity [2]. The core material has a low density, which gives it a relatively low weight, leading to sandwich panels with improved mechanical properties.

Sandwich panels are not only light in weight, but since the mid-20th century, they have been used as good sound and heat insulators [3]. Furthermore, sandwich panels have increased energy absorption capacity [4], high deflection resistance, bending stiffness, good impact resistance and high load withstanding [5]. These distinctive properties have earned it wide applications in areas such as aviation, automotive, and marine, in addition to building and construction applications, especially when lightweight is essential [6].

Sandwich panels, which consist of two or more layers of metal with a plastic core, spread widely, and many brands such as LITECOR[®], Usilight[®], Alucobond[®], Hylite[®], and Bondal[®] attracted researchers to conduct intensive studies [7]. These studies included single and multiple-stage mechanical joining [8], mortise-tenon mechanical joining [9], and spot welding [10, 11]. Several studies deal with LITECOR[®] sandwich panels, such as those investigating the tribological properties [12] and surface roughness [13].

Stiffening ribs are considered one of the essential improvements developed on structures because they effectively distribute the loads applied to the frame, which increases the load-bearing capacity and limits any potential deformations [14]. Several studies have attempted to strengthen sandwich panels by reinforcing them with additional stiffening ribs or making stiffening ribs within the same sandwich panel structure. Hand Lay-up, vacuum bagging, and resin infusion are the main techniques to stiffen sandwich panels and composite materials [15]. In the hand lay-up technique, sandwich panels are strengthened through stages where the mold is reinforced with fibers. Then a refractory resin is serially poured in a way that makes it uniformly distributed by using a brush until the required thickness is reached [16]. Vacuum bagging is an efficient method utilised to shape sandwich panels and composite materials. The composite materials' layers are laid on a mold to create a vacuum bag to compress the materials and remove air voids [17]. Resin infusion technology is a cost-effective and attractive process for shaping the complex geometries of composite materials, such as creating stiffing ribs. Sometimes it is called resin transfer molding, which includes injecting the resin into a preformed dry fiber preform seated in a mold under pressure to form the required ribs [18].

On the other hand, several studies using metal forming methods to form stiffening ribs in sandwich panels appeared recently, such as traditional stamping processes and incremental sheet forming (ISF), specifically single-point incremental forming (SPIF). The stamping technique in the punch-die is one of the most popular metal-forming technologies used to form materials in large quantities, especially sheet metal. It involves using a punch and a die to create the desired deformation through pressure [19]. While the punch is pressed all at once to create the required workpiece stamping, the ISF technique is often used in producing prototypes or producing limited quantities where the tool gradually forms the required workpieces [20, 21]. Because the ISF method is associated with CNC, the possibility of cracks in the workpiece is limited despite large plastic deformation [22].

The most popular incremental forming method (ISF) in recent years has been single-point incremental forming (SPIF). The SPIF used CNC to repeatedly generate a small, controlled deformation according to process parameters such as tool geometry and rotational speed, workpiece thickness, feed rate, and tool path [23]. Several recent attempts have used SPIF to strengthen sandwich panels and composite materials by creating stiffening ribs [24, 25].

Despite the wide range of studies that dealt with composite materials and sandwich panels, those dealing with the effects of stiffening ribs remained limited. Safiullin et al. [26] found the maximum localization of deformation and the local strain distribution of sandwich panels produced by titanium sheet alloy VT6S. They studied the reasons for the non-uniform thickness distribution near the holes in the stiffening ribs. Teodorescu et al. [27] studied the possibility of replacing the formal classic stiffening ribs in sandwich panels with two carbon/epoxy skins and a core of polystyrene reinforced with twill weave fabric for weight loss considerations. They compared the resulting stiffness with conventional sandwich panels.

In engineering applications that are exposed to external loads, internal stresses are often created, causing what is known as residual stresses (RS), which remain even after the removal of the effective loads [28]. The temperature gradient, the type of heat treatment, the properties of the materials, and the manufacturing methods are considered influential factors in generating RS. The residual stresses are generally considered a negative aspect of engineering structures, but they can be helpful in some applications [29, 30].

Sandwich panels and composite materials are no different from other structures, as residual stresses affect them positively and negatively depending on their applications. However, an excessive increase in residual stresses in these materials can lead to more significant deformation and dimension irregularities, negatively affecting the load-bearing capacity [31, 32]. Therefore, many studies have tried to understand residual stresses in composite materials better.

Incremental hole drilling, ring core, ultrasonic technique, and X-Ray Diffraction (XRD) are the main methods for measuring residual stresses in composite materials [33]. The hole-drilling technique indirectly measures residual stresses by drilling a small hole in the composite material to measure the strain relaxation around the hole with a strain gauge. The obtained values are used in theoretical equations or through calibration coefficients to find the residual stresses [34, 35]. It is important to note here that the drilling process may need more requirements related to the thickness of the layers of materials in sandwich panels [36]. The ring core method differs from the hole-drilling method in that it removes a ring core from the composite area and measures the resulting changes in the shape of the ring [37, 38]. This method is effective for measuring residual stresses in thin-layer applications [39]. Ultrasonic techniques depend on analyzing ultrasound data passing through composite materials, where residual stresses determines the spread of these waves. Therefore, the waves' behavior can indicate the presence or absence of residual stresses [40]. The residual stresses in XRD method is the tension brought on by the interaction of the tool used and the composite material surface. It depends on the variation of crystal lattice spacing, which can be widely used to calculate the residual stress distribution in composite materials [41].

In XRD, the residual stress is caused by the interaction between the shape-forming tool and the workpiece surface, where the average difference between the unclamped and clamped residual stress can reach 18% [42]. The XRD method is one of the most recently used to calculate residual stresses generated during metal forming. Maaß et al. [43] used this method to calculate bidirectional residual stresses in AA 5083 alloy sheets that SPIF formed. Tanaka et al. [44] also used it to investigate the impact of the SPIF tool's geometry, particularly the tool radius, on the generated RS.

Despite the increasing use of techniques for calculating residual stresses in composite materials, the qualitative use of calculating residual stresses for composite materials and sandwich panels strengthened by "stiffening ribs" is limited. The research gap in this field is still attractive to researchers and manufacturers alike.

The current study extends the authors' previous work studying residual stresses in Metal-Plastic composite stiffening ribs formed by SPIF using XRD [45]. This study uses the stamping method in the punch-die system to form the required stiffening ribs in Metal-Plastic Composites. Then it measures the residual stresses generated on both sides of the surface of the composite material in both the longitudinal and transverse axes. In addition, this study compares the effect of the stamping method in the punch-die system and the SPIF method on the residual stresses generated, giving it a novelty in the manufacture and design of sandwich panels and composite materials.

The remaining sections of this article focus on materials and methods, which include an explanation of how to use Materials and Methods in LITECOR® composite material and then an explanation of the X-ray Diffractometer to calculate residual stresses. In the results and discussion section, residual stress on the X and Y axes will be analysed, and the results obtained from the punch-die system method and the Single Point Incremental Forming (SPIF) method will be compared.

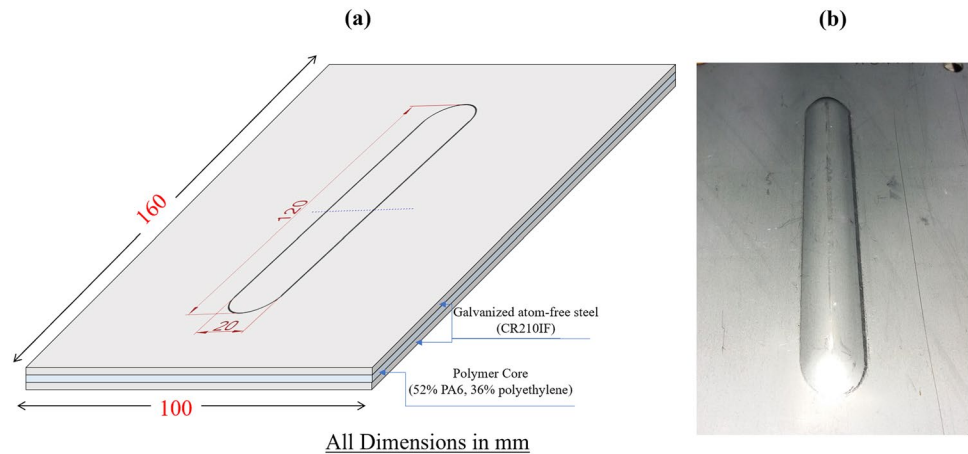
2 Materials and methods

This study investigates the residual stresses generated in Metal-Plastic Composites when they are strengthened by "stiffening ribs" using punch-die stamping technology. The XRD method was used to find the residual stresses at both ends of the LITECOR® composite material using a Proto iXRD Combo X-ray diffractometer at the Department of Materials Science at Rzeszów University of Technology.

2.1 Stiffening ribs forming

Three LITECOR® (ThyssenKrupp, Essen, Germany) metal-plastic composites of different core thicknesses were used in this study to investigate the RS. The LITECOR® is a sandwich panel consisting of three layers: two outer layers of galvanized atom-free steel (CR210IF) surrounding a polymer core of (52% PA6 and 36% polyethylene), as shown in Fig. 1a. The core thicknesses were 0.8, 1.25, and 1.6 mm, while the CR210IF thickness was constant. The LITECOR® sandwich panels have good mechanical properties, as yield strength ranges from 120 to 180 MPa, while Ultimate tensile strength can reach 240 MPa with elongation ratios over 25% [25].

Fig. 1 LITECOR® stamping
a workpiece dimensions,
b after stamping



The Zwick/Roell Z100 (ZwickRoell company, Ulm, Germany) testing machine equipped with compression test plates as a punch-die stamping system was used to form “20 mm wide, 120 mm long, 5 mm deep stiffening ribs” in the LITECOR® sandwich panel as shown in Fig. 1b.

2.2 X-ray diffraction diffractometer

The residual stresses measurements were completed utilizing a Proto iXRD Combo X-ray diffractometer. Since the 1960s, the $\sin 2\psi$ method has been considered the most crucial for measuring residual stresses when using the XRD technique [46]. So, it was used in this study to measure longitudinal and traverse components of generated residual stresses on both sides of the LITECOR® plastic-metal composite.

As indicated in Fig. 2, Eq. 1 determined strain in the measured direction [47]:

$$\epsilon_{\phi\psi} = \frac{1}{2}S_2(\sigma_{\phi})\sin^2\psi + \frac{1}{2}S_2(\tau_{\phi})\sin 2\psi - S_1(\sigma_{11} + \sigma_{22}) \quad (1)$$

where: normal stresses (σ_{11}, σ_{22}), shear stresses (τ_{ϕ}), stress component in measured direction (σ_{ϕ}), and X-ray elastic constants ($\frac{1}{2}S_2$ and S_1).

RS measurements were performed using the XRD $\sin 2\psi$ technique according to EN 15305:2008 and ASTM E915 standards. The measurement setup is shown in Fig. 3, where point 3 is in the centre of the plastic deformation area. Points 2 and 4 are within 5 mm, while 1 and 5 are within 25 mm distance from the centre point (3). residual stresses was determined on the surface in two axes, X and Y, perpendicular to each other. residual stresses Measurements were made on both sides of LITECOR® composite sheets.

Fig. 2 Plane-stress elastic model, diffracting crystallographic planes angle (ψ), normal stresses ($\sigma_{11}, \sigma_{22}, \sigma_{33}$), stress component in measured direction (σ_{ϕ})

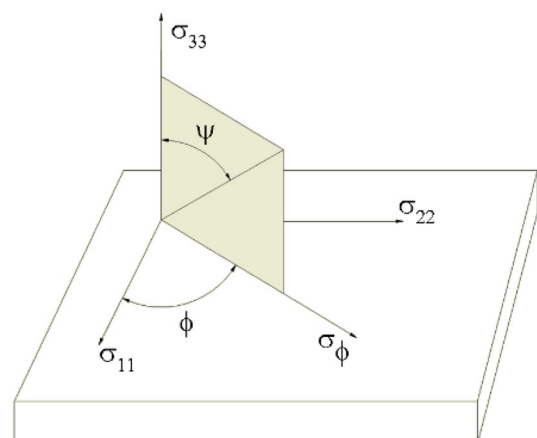
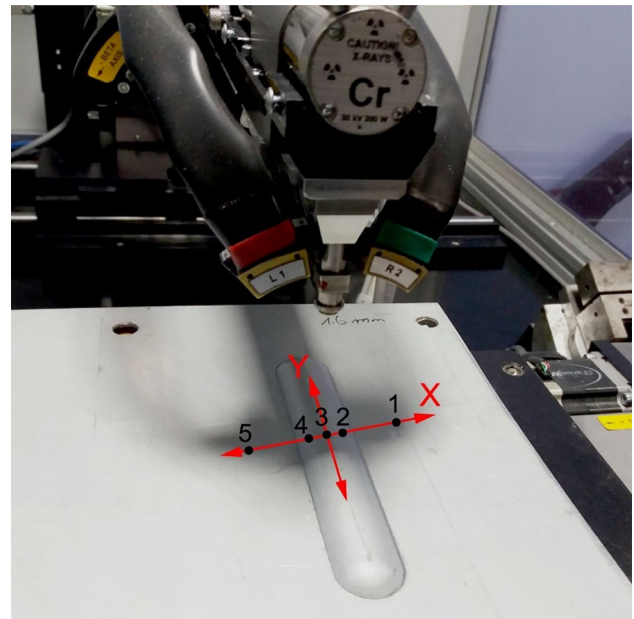


Fig. 3 LITECOR® stiffening rib with XRD setup



The Cr-K α X-ray tube was used as an XRD tool in the residual stresses measurements (wavelength λ , CrK α =0.2291 nm). Diffraction peaks of {211} crystal lattice planes were collected. The Bragg angle for the strain-free state was assumed as $2\theta = 156.4^\circ$. The strain was calculated using X-ray elastic constants of $\frac{1}{2}S_2 = 5.08 \times 10^{-6}$ MPa and $-S_1 = 1.27 \times 10^{-6}$ MPa. ψ angle values: $\pm 37.00^\circ$, $\pm 32.57^\circ$, $\pm 27.79^\circ$, $\pm 24.00^\circ$, $\pm 15.61^\circ$, $\pm 13.00^\circ$, $\pm 12.00^\circ$, $\pm 8.57^\circ$, $\pm 8.39^\circ$, $\pm 3.79^\circ$, and 0.00° . The rest process conditions were the following: aperture diameter – 2 mm, exposure time 2 s, gain material β -Ti, number of exposures per ψ angle – 15, X-ray tube power – 80 W ($U = 20$ kV, $I = 4$ mA), Gaussian peak fit.

3 Results and discussions

LITECOR® polymer-metal composite consisting of a polymer core layer and two outer layers of galvanized steel was used in this study, where the XRD method was used for measuring the residual stresses in the formed “stiffening ribs” by the punch-die stamping technology. Three core thicknesses were examined according to the generated RS. The residual stresses were measured for the front and back sides of the LITECOR® for both x-and y axes. The selected core thicknesses are 0.8 mm, 1.25 mm, and 1.6 mm. For each core thickness, five points 1, 2, 3, 4 and 5 were examined at distances 25, 5, 0, -5, and -25 mm, respectively. The resulting residual stresses are indicated in Table 1. Figures 4, 5, 6 and 7 show the changes in the residual stresses on the “stiffening ribs” for both the X and Y axes.

3.1 Residual stress in X-axis

Figure 4 shows the change in residual stresses depending on the locations of the five pre-selected x-axis measuring points on the front side of the LITECOR® material. In the case of thickness 0.8 mm, the value of residual stresses in the central point (3) was about 1020 MPa. It decreased symmetrically in points 2 and 4, which can be attributed to the redistribution of forces within the structure in the formed stiffening ribs, where the stress decreases when it becomes more uniform. For points 1 and 5, there is a noticeable increase in RS, reaching about 1200 MPa, where these points suffer from an increase in the concentration of stresses and external loading. The matter was different for the two cases of core thickness 1.25 and 1.6 mm, as the lowest values of residual stresses were generated at the central points. Hence, there was a steady increase whenever it moved away from the central point, which can be attributed to the fact that these points can have a higher load.

Generally, residual stress values decrease for the anterior aspect with increasing core thickness. Changes in stiffness and stress concentration could explain the resulting behaviour. According to stiffness, the decrease in the thinner thickness plays a role in reducing the stiffness of the composite material. Therefore, an increase in Stress Concentration can

Table 1 residual stresses for the X and Y axes of the LITECOR® stiffening rib

Core thickness (mm)	Points	Distance (mm)	Residual Stress MPa (Front Side)		Residual Stress MPa (Back Side)	
			X-axis	Y-axis	X-axis	Y-axis
0.8	1	25	1195	1199	1052	1025
0.8	2	5	835	1056	934	998
0.8	3	0	1020	1060	1146	1055
0.8	4	-5	852	1027	1012	1083
0.8	5	-25	1198	1120	1075	1034
1.25	1	25	913	977	1037	1020
1.25	2	5	914	1048	894	980
1.25	3	0	786	849	895	930
1.25	4	-5	816	1087	812	841
1.25	5	-25	895	969	985	894
1.6	1	25	589	1038	1119	1178
1.6	2	5	601	1085	921	951
1.6	3	0	531	593	970	925
1.6	4	-5	660	995	897	871
1.6	5	-25	650	993	1040	1045

Fig. 4 Residual stress of x-axis of LITECOR® stiffening rib (front side)

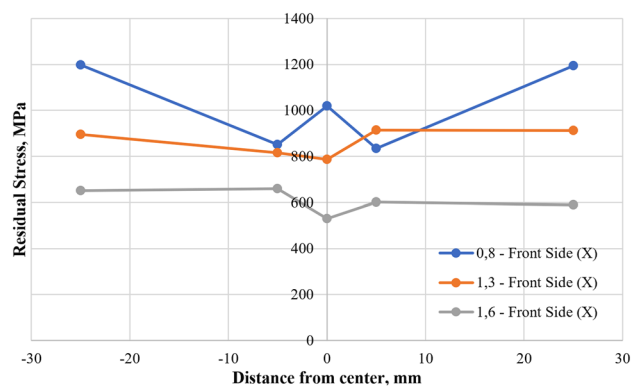
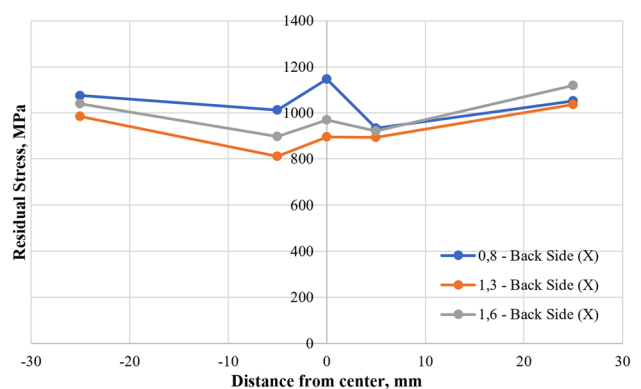


Fig. 5 Residual stress of x-axis of LITECOR® stiffening rib (back side)



occur within the “stiffened ribs” formed due to the decrease in the ability of the core to absorb loads, which leads to an increase in the residual stresses to absorb the applied forces.

In contrast, the values of the residual stresses on the back side of the “stiffened ribs” can be considered as values corresponding to the values of the front side with two things in mind, as shown in Fig. 5. The values at the central points on the front side are relatively higher than the corresponding values on the back side, and the core with a thickness of 1.6 mm gave higher residual stresses than those achieved with a thickness of 1.25 mm. The differences between the front

Fig. 6 Residual stress of y-axis of LITECOR® stiffening rib (front side)

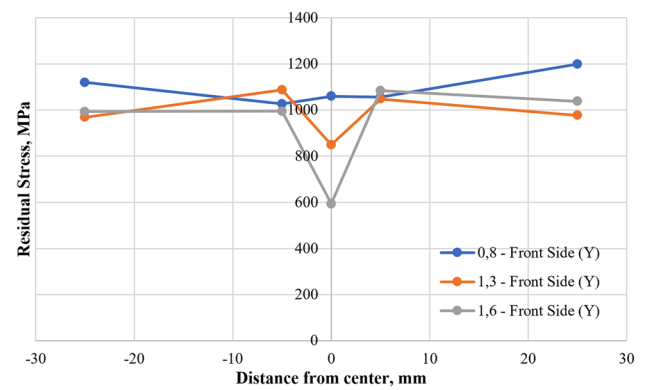
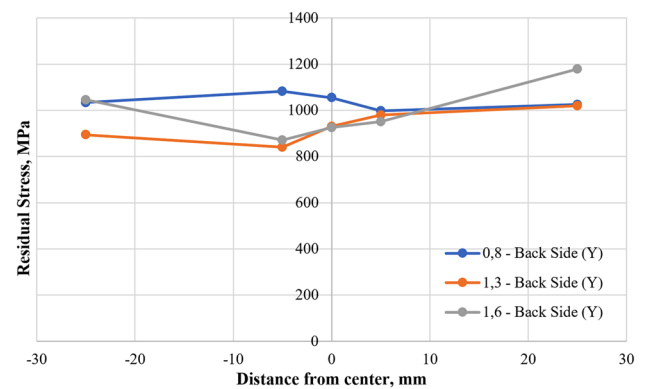


Fig. 7 Residual stress of y-axis of LITECOR® stiffening rib (back side)



and back sides can be attributed to the deformation mechanism and material flow during forming of stiffening ribs by punching on the LITECOR® composite. The difference in the deformation and the material flow leads to heterogeneity in the distribution of the residual stresses and their concentration at specific points and on one side at the expense of the other. This result explains the higher values in the central points on the back side on the computation of their counterparts on the front side and the high stresses at a LITECOR® core of 1.6 mm, which are higher than those achieved in 1.25 mm core thickness.

3.2 Residual stress in Y-axis

Regarding the residual stresses in the y-axis, Figs. 6 and 7 represent the change in the residual stresses at the selected points 1–5 for both the front and back sides, respectively. When the thickness of the core was 0.8 mm, it was observed that the residual stresses on the anterior side were relatively high when compared to the x-axis, as they ranged between 1027 MPa and 1199 MPa and were also higher than those achieved on the back side (998 MPa to 1083 MPa). When the thickness of the core was 1.25 mm, the behaviour of the composite material towards the residual stresses in the y-axis was similar to that of the x-axis, whether it was on the front side or the back side of the core. It was clear that the lowest residual stresses were found in the central point (0), while points 1 and 5 were slightly higher, and the values were similar for the y-axis for both sides, where they were 849 MPa to 1087 MPa for the anterior side and 841 MPa to 1020 MPa for the backside.

Concerning the maximum thickness of the core used in this study, the behaviour continued similarly to the previous cases in the frontal aspect, as the residual stress in the y-axis is highest at distal terminal points 1 and 5. At the same time, the lowest values are achieved at the central point (0). It can also be noted that the values on the back side exceeded those on the front side, reaching 871–1178 MPa.

In sum, there is consistency in the general stress distribution patterns when comparing the values achieved between the y-axis and x-axis for both sides of the stiffening ribs. Despite this, some differences can be observed that may occur due to several factors, such as the interference in the LITECOR® composite material's layers between the core and the two outer layers or the asymmetry that occurs in the formed material.

It is worth noting that the values of the residual stresses on both sides and in both axes exceeded the tensile strength values for LITECOR sandwich samples in some cases. This fact can be explained by several aspects, such as that residual stresses are typically measured using non-destructive techniques such as X-ray diffraction. These techniques provide insight into the internal stress state of the material. Regardless, they do not directly demonstrate the stress that would cause a fracture. Residual stresses can be addressed within a composite material without causing immediate failure because they are balanced by compressive stresses in other regions or due to material constraints. Comparing residual stresses with static tensile yield strength can be misleading, primarily because the stress states in these two scenarios differ significantly. The forming process introduces complex stress distributions within LITECOR composite materials, especially in the sandwich samples. While uniaxial tension is applied during a tensile test, the forming process subjects the composite to multi-axial loading, making distinct stress components [48].

Furthermore, residual stresses can endure due to the material's elastic deformation, which continues even after the composite layers are bonded and deformed. It is essential to recognize that a substantial reduction in tensile stresses typically happens when the layers of the LITECOR tile are separated and the elastic deformation disperses. As a result, differences in stress values are pronounced between thinner (0.8 mm) and thicker (1.6 mm) sheets. Moreover, the choice of diffraction elastic constants (XEC) used in X-ray diffraction (XRD) measurements is a contributing factor, which can have a modest impact on calculated stress values, typically up to approximately 150 MPa. In some instances, tensile stresses may exceed yield strength, especially after processes that induce high tensile stresses, highlighting the unique behavior of composite materials under complex loading conditions. The current study focused on a composite sandwich strengthened by stiffening ribs, where the stiffening ribs increased the material strength by around 35% [49].

3.3 Effect of forming methods

To demonstrate the effect of forming processes on the quality of the resulting "stiffening ribs", this study focuses on the residual stress aspect, which is paramount in future failure processes. The study evaluated the results obtained from the "stiffening ribs" method using the stamping method in the punch-die system. Furthermore, it compared them with those previously obtained using the SPIF method [45].

Table 2 compares the residual stress values obtained using both methods for the x-axis, whether for the front and back sides for all used core thicknesses (0.8, 1.25, and 1.6) and compares the maximum and minimum values for each case. In contrast, Table 3 indicates what was obtained for the y-axis.

The results of the front side of the x-axis showed that the minimum residual stress values were obtained using the SPIF method compared to the stamping punch method. This result may be because the SPIF method relies on incremental deformation, facilitating controlled material flow, leading to low plastic deformation and, thus, lower residual stress values at all points of stiffening ribs in LITECOR® composite material. Moreover, the maximum residual stresses were achieved

Table 2 Comparing between stamping punch and SPIF methods for X axis Residual stresses

Side	Distance (mm)	Stamping punch method Residual stress (MPa)			SPIF method Residual stress (MPa) [45]		
		t=0.8	t=1.25	t=1.6	t=0.8	t=1.25	t=1.6
Front side	25	765	736	801	1195	913	589
	5	395	345	-75	835	914	601
	0	473	494	557	1020	786	531
	-5	488	187	-166	852	816	660
	-25	879	711	651	1198	895	650
	Min	395	187	-166	835	786	531
	Max	879	736	801	1198	914	660
Back Side	25	1041	755	956	1052	1037	1119
	5	-193	-246	-164	934	894	921
	0	784	753	509	1146	895	970
	-5	-224	-124	-176	1012	812	897
	-25	1004	762	957	1075	985	1040
	Min	-224	-246	-176	934	812	897
	Max	1041	762	957	1146	1037	1119

Table 3 Comparing between stamping punch and SPIF methods for Y axis Residual stresses

Side	Distance (mm)	Stamping Punch Method Residual Stress (MPa)			SPIF Method Residual Stress (MPa) [45]		
		t=0.8	t=1.25	t=1.6	t=0.8	t=1.25	t=1.6
Front side	25	1199	977	1038	790	816	759
	5	1056	1048	1085	536	436	257
	0	1060	849	593	557	525	384
	-5	1027	1087	995	483	422	283
	-25	1120	969	993	857	784	684
	Min	1027	849	593	483	422	257
	Max	1199	1087	1085	857	816	759
Back Side	25	1025	1020	1178	1130	869	932
	5	998	980	951	92	141	21
	0	1055	930	925	1260	830	678
	-5	1083	841	871	158	208	112
	-25	1034	894	1045	1062	819	937
	Min	998	841	871	92	141	21
	Max	1083	1020	1178	1260	869	937

using the stamping punch method, especially at core thicknesses of 0.8 and 1.6 mm, with values close between the two methods at 1.25 mm thickness. The higher stress concentration and plastic deformation due to the rapid forming process used in the stamping punch method are the main reasons for higher values than the SPIF method. For the back side, the matter did not differ from the front side, as the highest values of residual stresses were achieved using the stamping method compared to the SPIF method.

When the residual stress values are observed in the y-axis, the comparisons between the two methods generally indicate that the SPIF method gives lower stress values for all core thicknesses than the stamping method. These results favour using the SPIF method in forming stiffening ribs in LITECOR® composite material when obtaining the lowest residual stress is a target.

These results are crucial when using sandwich panels, especially regarding structural integrity and generally affect the final product's performance.

4 Conclusions

This study aimed to investigate the distribution of residual stresses in stiffening ribs created by the stamping method in the punch-die system in several composite panels consisting of a core of polymer and two outer layers of steel, depending on the thickness of the core layer. The two-dimensional X-ray diffraction (XRD) method measured the residual stresses at five selected points on both the anterior and posterior sides. Then the study compared these values with previously obtained using the single point incremental formation (SPIF). Among the most critical conclusions obtained:

- The thickness of the core plays a prominent role in the resulting residual stresses, as the values decreased as the thickness of the core increased for both the anterior and posterior sides and for both the x- and y-axes.
- The values of the residual stresses differ depending on the location of the five selected points, especially between the central and those points on their right and left sides.
- When comparing the two axes, the values measured on the y-axis are generally higher than the corresponding values on the x-axis on the anterior sides, as they ranged between 1027 MPa and 1199 MPa, or the back side (998 MPa to 1083 MPa) at a core thickness of 0.8 mm.
- When comparing the residual stresses obtained from the stamping method in the punch-die system with those previously obtained from using the SPIF method, the SPIF method gives residual stress values that are much lower than the stamping method, which makes it preferable, especially when the target is the lowest possible stresses.

Author contributions Conceptualization, RA-S and AK; methodology, AK, AG, MK, RA-S and HIK; investigation, AK, RA-S, AG and HIK; resources, JS, RA-S and AK; writing—original draft preparation, RA-S; writing—review and editing, RA-S; supervision, RA-S, KO and AK; project administration, RA-S, JS, AK and KO. All authors have read and agreed to the published version of the manuscript.

Funding The authors are grateful for the support in the experimental work to the Grant Agency of the Ministry of Education, Science, Research, and Sport of the Slovak Republic (grant number VEGA 1/0539/23). Thanks for the support also to the Polish National Agency for Academic Exchange, project title: “Research on the possibilities of forming and joining innovative metal-plastic composites in the production of light-weight thin-walled structures”, project number: BPN/BSK/2023/1/00038/U/00001.

Data availability All data generated or analyzed during this study are included in this published article.

Declarations

Competing interests The authors declare no competing interests.

Open Access This article is licensed under a Creative Commons Attribution 4.0 International License, which permits use, sharing, adaptation, distribution and reproduction in any medium or format, as long as you give appropriate credit to the original author(s) and the source, provide a link to the Creative Commons licence, and indicate if changes were made. The images or other third party material in this article are included in the article's Creative Commons licence, unless indicated otherwise in a credit line to the material. If material is not included in the article's Creative Commons licence and your intended use is not permitted by statutory regulation or exceeds the permitted use, you will need to obtain permission directly from the copyright holder. To view a copy of this licence, visit <http://creativecommons.org/licenses/by/4.0/>.

References

1. Castanie B, Bouvet C, Ginot M. Review of composite sandwich structure in aeronautic applications. *Compos Part C Open Access*. 2020. <https://doi.org/10.1016/j.jcomc.2020.100004>.
2. Foraboschi P. Three-layered sandwich plate: exact mathematical model. *Compos B Eng*. 2013. <https://doi.org/10.1016/j.compositesb.2012.08.003>.
3. Lange J, von der Heyden A, Grimm S. Sandwich panels in buildings: core, structure and design. In: *Advances in engineering materials, structures and systems: innovations, mechanics and applications—proceedings of the 7th international conference on structural engineering, mechanics and computation*, 2019; 2019. <https://doi.org/10.1201/9780429426506-157>
4. Zhang Z, Lei H, Xu M, Hua J, Li C, Fang D. Out-of-plane compressive performance and energy absorption of multi-layer graded sinusoidal corrugated sandwich panels. *Mater Des*. 2019. <https://doi.org/10.1016/j.matdes.2019.107858>.
5. Kang L, Sun C, An F, Liu B. A bending stiffness criterion for sandwich panels with high sound insulation and its realization through low specific modulus layers. *J Sound Vib*. 2022. <https://doi.org/10.1016/j.jsv.2022.117149>.
6. Wendel E. Evaluation of potential for metal/polymer/metal sandwich material as outer panels for trucks. 2019.
7. Contreiras TRM. Joining by forming of composite sandwich panels, Master, Superior Técnico, Lisboa, 2019. [Online]. Available: <https://fenix.tecnico.ulisboa.pt/downloadFile/1126295043836505/Thesis.pdf>.
8. Contreiras TRM, Pragana JPM, Bragança IMF, Silva CMA, Alves LM, Martins PAF. Joining by forming of lightweight sandwich composite panels. In: *Procedia manufacturing*; 2019. <https://doi.org/10.1016/j.promfg.2019.02.140>
9. Pragana JPM, Contreiras TRM, Bragança IMF, Silva CMA, Alves LM, Martins PAF. Joining by forming of metal–polymer sandwich composite panels. *Proc Inst Mech Eng B J Eng Manuf*. 2019. <https://doi.org/10.1177/0954405418815386>.
10. Kustroń P, Korzeniowski M, Piwowarczyk T, Sokołowski P. Development of resistance spot welding processes of metal–plastic composites. *Materials*. 2021. <https://doi.org/10.3390/ma14123233>.
11. Naimi IKA. Weldability of new material sandwich steel for automotive applications. *Al-Khwarizmi Eng J*. 2016;12(2):60–78.
12. Trzepieciński T, Kubit A, Slota J. Assessment of the tribological properties of the steel/polymer/steel sandwich material LITECOR. *Lubricants*. 2022;10(5):99. <https://doi.org/10.3390/lubricants10050099>.
13. Al-Sabur R, Kubit A, Khalaf H, Jurczak W, Dzierwa A, Korzeniowski M. Analysis of surface texture and roughness in composites stiffening ribs formed by SPIF process. *Materials*. 2023;16(7):2901. <https://doi.org/10.3390/ma16072901>.
14. Shen L, et al. Experimental study on the behavior of a novel stiffened hexagonal CFDST stub column under axial load. *J Struct Eng*. 2022. [https://doi.org/10.1061/\(asce\)st.1943-541x.0003198](https://doi.org/10.1061/(asce)st.1943-541x.0003198).
15. Ashrith HS, Jeevan TP, Xu J. A review on the fabrication and mechanical characterization of fibrous composites for engineering applications. *J Compos Sci*. 2023;7(6):252. <https://doi.org/10.3390/jcs7060252>.
16. Yahaya R, Sapuan SM, Jawaid M, Leman Z, Zainudin ES. Investigating ballistic impact properties of woven kenaf-aramid hybrid composites. *Fibers Polym*. 2016. <https://doi.org/10.1007/s12221-016-5678-6>.
17. Dong X, Chen K, Xue P, Cui Y, Jia M. Optimization of process parameters for the preparation of continuous glass fiber-reinforced Nylon 6 composites by vacuum bagging process. *J Appl Polym Sci*. 2022. <https://doi.org/10.1002/app.53005>.
18. Ravindran B, Feuchter M, Schledjewski R. Investigation of the mechanical properties of sandwich composite panels made with recycled flax fiber/bio-based epoxy processed by liquid composite molding. *J Compos Sci*. 2023. <https://doi.org/10.3390/jcs7030122>.
19. Qattawi A, Mayyas A, Dongri S, Omar M. Knowledge-based systems in sheet metal stamping: a survey. *Int J Comput Integr Manuf*. 2014. <https://doi.org/10.1080/0951192X.2013.834463>.

20. Cao T, et al. An efficient method for thickness prediction in multi-pass incremental sheet forming. *Int J Adv Manuf Technol.* 2015;77:1–4. <https://doi.org/10.1007/s00170-014-6489-9>.
21. Ingarao G, di Lorenzo R, Micari F. Sustainability issues in sheet metal forming processes: an overview. *J Clean Prod.* 2011. <https://doi.org/10.1016/j.jclepro.2010.10.005>.
22. Ai S, Lu B, Chen J, Long H, Ou H. Evaluation of deformation stability and fracture mechanism in incremental sheet forming. *Int J Mech Sci.* 2017. <https://doi.org/10.1016/j.ijmecsci.2017.03.012>.
23. Krasowski B, Kubit A, Trzepieciński T, Dudek K, Slota J. Application of X-ray diffraction for residual stress analysis in truncated cones made by incremental forming. *Adv Sci Technol Res J.* 2020. <https://doi.org/10.12913/22998624/118829>.
24. Trzepieciński T, Kubit A, Dzierwa A, Krasowski B, Jurczak W. Surface finish analysis in single point incremental sheet forming of rib-stiffened 2024-T3 and 7075-T6 clad aluminium alloy panels. *Materials.* 2021. <https://doi.org/10.3390/ma14071640>.
25. Kubit A, Korzeniowski M, Bobusia M, Ochałek K, Slota J. Analysis of the possibility of forming stiffening ribs in Litecor metal-plastic composite using the single point incremental forming method. In *key engineering materials. Trans Tech Publ;* 2022. pp. 802–14.
26. Safiullin RV, Rudenko OA, Enikeev FU, Lutfullin RY. Superplastic forming of sandwich cellular structures from titanium alloy. *Mater Sci Forum.* 1997. <https://doi.org/10.4028/www.scientific.net/msf.243-245.769>.
27. Teodorescu-Draghicescu H, Vlase S, Luca DM, Scutaru ML, Stanciu A, Rosu D. New ultra lightweight and extreme stiff sandwich composite structure for multiple applications. In: *Annals of DAAAM and proceedings of the international DAAAM symposium, danube adria association for automation and manufacturing, DAAAM, 2008*, pp. 1375–1376.
28. Zaghaj J, Mertinger V, Filep A, Varga G, Benke M. Characterization of residual stresses induced into bearing rings by means of soft turning using different turning parameters. *J Mach Eng.* 2021. <https://doi.org/10.36897/jme/144299>.
29. Tabatabaeian A, Ghasemi AR, Shokrieh MM, Marzbanrad B, Baraheni M, Fotouhi M. Residual stress in engineering materials: a review. *Adv Eng Mater.* 2022. <https://doi.org/10.1002/adem.202100786>.
30. Withers PJ, Bhadeshia HKDH. Residual stress part 2—nature and origins. *Mater Sci Technol.* 2001. <https://doi.org/10.1179/026708301101510087>.
31. Chava S, Namilae S. Continuous evolution of processing induced residual stresses in composites: an in-situ approach. *Compos Part A Appl Sci Manuf.* 2021. <https://doi.org/10.1016/j.compositesa.2021.106368>.
32. Parlevliet PP, Bersee HEN, Beukers A. Residual stresses in thermoplastic composites—a study of the literature. Part III: effects of thermal residual stresses. *Compos Part A Appl Sci Manuf.* 2007. <https://doi.org/10.1016/j.compositesa.2006.12.005>.
33. Lunt AJG, et al. A state-of-the-art review of micron-scale spatially resolved residual stress analysis by FIB-DIC ring-core milling and other techniques. *J Strain Anal Eng Des.* 2015. <https://doi.org/10.1177/0309324715596700>.
34. Sicot O, Gong XL, Cherouat A, Lu J. Determination of residual stress in composite laminates using the incremental hole-drilling method. *J Compos Mater.* 2003. <https://doi.org/10.1177/002199803031057>.
35. Liu X, Wang X, Guan Z, Jiang T, Geng K, Li Z. Improvement and validation of residual stress measurement in composite laminates using the incremental hole-drilling method. *Mech Mater.* 2021. <https://doi.org/10.1016/j.mechmat.2020.103715>.
36. Vasylevskiy K, Tsukrov I, Drach B, Buntrock H, Gross T. Identification of process-induced residual stresses in 3D woven carbon/epoxy composites by combination of FEA and blind hole drilling. *Compos Part A Appl Sci Manuf.* 2020. <https://doi.org/10.1016/j.compositesa.2019.105734>.
37. Ghaedamini R, Ghassemi A, Atrian A. Ring-core method in determining the amount of non-uniform residual stress in laminated composites: experimental, finite element and theoretical evaluation. *Arch Appl Mech.* 2018. <https://doi.org/10.1007/s00419-017-1340-z>.
38. Umarfarooq MA, Shivakumargouda PS, Veeresh Kumar GB, Kodancha KG. An assessment on the residual stress measurement in FRP composites using relaxation techniques. *Iran J Mater Sci Eng.* 2021. <https://doi.org/10.22068/ijmse.2075>.
39. Gao H, Li X, Wu Q, Lin M, Zhang Y. Effects of residual stress and equivalent bending stiffness on the dimensional stability of the thin-walled parts. *Int J Adv Manuf Technol.* 2022;119:7–8. <https://doi.org/10.1007/s00170-021-08252-3>.
40. Song W, Xu C, Pan Q, Song J. Nondestructive testing and characterization of residual stress field using an ultrasonic method. *Chin J Mech Eng (Engl Edit).* 2016. <https://doi.org/10.3901/CJME.2015.1023.126>.
41. Epp J. X-Ray Diffraction (XRD) Techniques for Materials Characterization, in *Materials Characterization Using Nondestructive Evaluation (NDE) Methods*, 2016. <https://doi.org/10.1016/B978-0-08-100040-3.00004-3>.
42. Maaß F, Gies S, Dobecki M, Brömmelhoff K, Tekkaya AE, Reimers W. Analysis of residual stress state in sheet metal parts processed by single point incremental forming. In: *AIP conference proceedings*, 2018. <https://doi.org/10.1063/1.5035043>.
43. Maaß F, Hahn M, Dobecki M, Thannhäuser E, Tekkaya AE, Reimers W. Influence of tool path strategies on the residual stress development in single point incremental forming. In: *Procedia manufacturing*; 2019. <https://doi.org/10.1016/j.promfg.2019.02.105>.
44. Tanaka S, Nakamura T, Hayakawa K, Nakamura H, Motomura K. Residual stress in sheet metal parts made by incremental forming process. In: *AIP conference proceedings*; 2007. <https://doi.org/10.1063/1.2740904>.
45. Kubit A, Al-Sabur R, Gradzik A, Ochałek K, Slota J, Korzeniowski M. Investigating residual stresses in metal-plastic composites stiffening ribs formed using the single point incremental forming method. *Materials.* 2022;15(22):8252. <https://doi.org/10.3390/ma15228252>.
46. GUO J, FU H, PAN B, KANG R. Recent progress of residual stress measurement methods: a review. *Chin J Aeronaut.* 2021. <https://doi.org/10.1016/j.cja.2019.10.010>.
47. Kocurek P. Analiza stanu naprężeń własnych w odlewach segmentu aparatu kierującego turbiny silników lotniczych. *Inżynieria Materiałowa.* 2015. <https://doi.org/10.15199/28.2015.3.7>.
48. M'Saoubi R, Outeiro JC, Changeux B, Lebrun JL, Morão A, Dias. Residual stress analysis in orthogonal machining of standard and resulfurized AISI 316L steels. *J Mater Process Technol.* 1999;96:1–3. [https://doi.org/10.1016/S0924-0136\(99\)00359-3](https://doi.org/10.1016/S0924-0136(99)00359-3).
49. Kubit A, Trzepieciński T, Krasowski B, Slota J, Spišák E. Strength analysis of a rib-stiffened glare-based thin-walled structure. *Materials.* 2020. <https://doi.org/10.3390/ma13132929>.